Polymer 146 (2018) 312–320

Contents lists available at ScienceDirect

Polymer

journal homepage: www.elsevier.com/locate/polymer

Electrochemical sensing and nano molar level detection of Bisphenol-A with molecularly imprinted polymer tailored on multiwalled carbon nanotubes

T.S. Anirudhan*, V.S. Athira, V. Chithra Sekhar

Department of Chemistry, School of Physical and Mathematical Sciences, University of Kerala, Kariavattom, Trivandrum, 695 581, India

ARTICLE INFO

Article history:
Received 22 December 2017
Received in revised form
11 May 2018
Accepted 18 May 2018
Available online 18 May 2018

Keywords:
Bisphenol A
Multiwalled carbon nanotube
Molecularly imprinted polymer
Electrochemical sensing
Nano molar detection

ABSTRACT

A rapid, effective and simple method for quantitative determination of Bisphenol-A (BPA) is important in environmental monitoring and health perspectives. In this work, a multi-walled carbon nanotube (MWCNT) based molecularly imprinted polymer (MIP) was successfully developed and used for modifying glassy carbon electrode (GCE) for the electrochemical detection of BPA. FTIR, Raman, XRD, SEM and AFM techniques were used for confirming the stepwise modifications in each stage. A well defined electrochemical response was obtained for BPA in cyclic voltammetry and differential pulse voltammetry. The influence of accumulation time and pH was studied and optimized. The electro catalytic sensing of BPA is possible with accessible range from 400.00 μM to 0.10 nM with detection limit of 0.02 nM. The stability, reproducibility and repeatability of the MIP/GCE sensor were also investigated. The applicability of the synthesized sensor in real life situation was confirmed by quantifying the amount of BPA in baby feeding bottle extracts.

© 2018 Elsevier Ltd. All rights reserved.

1. Introduction

Bisphenol A (BPA) or [2,2-bis (4-hydroxyphenyl)propane] is an essential ingredient in the production of various consumer products hence humans are widely exposed to this toxic chemical. The main sources of BPA in food and environment are polycarbonates (infant feeding bottles, microwave ovenware, storage containers, reusable water and milk bottles and water pipes), epoxy resins (internal protective lining for food containers and beverage cans), unsaturated polyester resins and polysulfones [1]. Being an endocrine disrupting chemical, BPA affects many physiological processes. BPA exposures have been associated with female and male reproductive failure, obesity, diabetes, skin sensitization, immune system failure, thyroid dysfunction, diverse pleiotropic actions in the brains and cardiovascular system and carcinogenesis of the prostate and breast [2]. Recent reports reveal that even at low doses of BPA in nano molar level lead the disruption of the cell function [3]. Hence the accurate determination of trace level of BPA is having research interest in the present scenario.

Different methods have been reported for detecting BPA, such as spectrophotometry, gas chromatography coupled with mass spectroscopy, high performance liquid chromatography, enzyme-linked immunosorbent assay, and electrochemical method [4]. Some of these strategies suffer from disadvantages including the involvement of time-consuming manipulation steps, requirement of special instrumentation and skilled personals, consumption of a large amount of organic reagents etc. Electrochemical sensing technique is among the most facile and promising approaches for BPA detection as it providing advantageous such as sensitivity, ease of use, potential for miniaturization, low cost and on-line monitoring capabilities. The direct electrochemical detection of BPA at traditional carbon and metal electrodes suffers from disadvantages including attenuated signal, reduced sensitivity and reproducibility over time, which are due to surface fouling and passivation [5,6].

As a key component in the sensor system, different strategies have been reported for the modification of sensor electrode. Molecularly imprinted technique (MIT) is an effective approach for modifying electrode to improve sensitivity and selectivity of the sensor system. MIT produces a polymeric network with specific binding site for analyte molecule. This polymeric network with predetermined recognition capacity to a particular analyte can be used as a sensitive tool for its determination [7]. Molecularly imprinted polymers (MIP) are prepared by the polymerization of

* Corresponding author.
E-mail address: tsani@rediffmail.com (T.S. Anirudhan).

https://doi.org/10.1016/j.polymer.2018.05.052
0032-3861/© 2018 Elsevier Ltd. All rights reserved.

functional monomers and cross linkers in the presence of template molecule followed by template extraction from the polymer network leaving specific binding sites [8,9]. Conventional MIPs possess drawbacks such as low binding efficiency, poor site accessibility, complicated fabrication processes and slow binding kinetics. Synthesis of MIP on the surface of a support material (surface imprinting) is a convenient method to overcome these shortcomings [10]. Among the multifarious imprinting support materials, nanostructured materials possess small dimension with extremely high surface area to volume ratio, easiest template binding and rebinding capacity and faster binding kinetics. Thus materials including mesoporous silica [11], graphene based nanomaterials [12], gold nanoparticles [13], TiO_2 nanotubes [14] and carbon nanotube (CNT) with nanoscale and porous features have been reported for electrode modification. Among these, CNTs with unique physiochemical properties, fast electron transfer kinetics and extremely large surface area would therefore proposed to be an excellent candidate as a support material for preparing imprinted materials for sensor fabrication [15]. To obtain surface imprinted polymer on CNT with improved properties, synthetic efforts have been devoted towards the surface functionalization. Surface coating of CNT using surfactant molecule maintain the integrity of CNT and its conjugated backbone compared to covalent side wall functionalization. Coating CNT with porous silica is one of the most attractive concepts to improve the dissolution and electro catalytic properties [16,17]. The silica coated CNT draw the attention of researchers in the field of electrochemical sensors as it can display a synergistic effect of catalytic property of porous silica and electrical conductivity of CNT [18].

In the present work, a novel MIP was synthesized on the surface of silica coated CNTs for the electrochemical determination of BPA. A bifunctional silylating agent glycidoxy propyl trimethoxy silane (GLYMO), with organic epoxide and hydrolysable methoxysilyl groups was used to achieve excellent mechanical and adhesion properties [19]. Vinyl functionalization was done by grafting with allyl amine (AA). MIP was prepared in an easy and conventional way by co-polymerization of functional monomers vinylpyridine (4-VPy) and methacrylic acid (MAA) with cross-linker ethylene glycol dimethylacrylate (EDGMA). In addition to the H-bonding interaction offered by both the monomers, the π-π stacking interaction between pyridinyl and phenyl ring contribute to better selectivity and sensitivity of the prepared MIP. Modifications in each stage of synthesis of MIP were confirmed through systematic characterization using FTIR, Raman, XRD, AFM and SEM techniques. The electrochemical behaviors of the modified electrode were investigated by cyclic voltammetry (CV) and differential pulse voltammetry (DPV). The dispersed MIP is drop-casted into the glassy carbon electrode (GCE) surface, after which the electrodes are used for electrochemical sensing. The MIP/GCE found to exhibit greater stability and reproducibility for determination of BPA in aqueous buffer solution of pH 7.0 over non-imprinted polymer (NIP) and bare GCEs. In the represent investigation, a novel electrochemical sensing platform has been successfully employed to recognize and detect BPA in baby feeding bottles.

2. Materials and methods

2.1. Materials

MWCNTS were purchased from Shenzhen Nanotechnologies Co.Ltd. Analytical grade chemicals were used for all the analysis without further purification. MAA, 4-VPy, AA, bisphenol F (BPF), phenol (Ph), and 1,4-dihydroxybenzene(DHB), EGDMA, tetraethoxysilane (TEOS), chitosan and potassium ferricyanide ($K_3[Fe(CN)_6]$) were purchased from E-Merk, India Ltd. BPA, GLYMO, cetyl trimethyl ammonium bromide (CTAB), N, N′- Dicyclohexylcarbodiimide (DCC) and 2,2-azobis isobutyronitrile (AIBN) were obtained from Alfa Aesar. The electrochemical measurements were performed in phosphate buffer solution (0.10 M) and were prepared by mixing 0.10 M NaH_2PO_4 and 0.10 M Na_2HPO_4 and adjusting the pH. All other solvents used were purchased from Merck and were used as received.

2.2. Equipments and methods of characterization

Perkin Elmer 1800 model FT-IR spectrometer was used for performing the IR characterization of samples, wave number range from 600 to 4000 cm^{-1}. The pH measurements were made on Systronics μ pH meter (Model 361). Raman spectra of the prepared samples were collected using the micro Raman spectrometer Lab Ram UV HR, Jobin Yvon. X-ray diffraction (XRD) patterns of the samples were examined using Siemens D5005 X- Ray unit. Scanning electron microscopy (SEM) measurements were carried out using Carl Zeiss EVO-18 scanning electron microscope operated in vacuum at 15–20 kV and having a working distance of 12 mm using a secondary ion detector. Atomic force microscope (AFM) images were recorded on Bruker DIMENSION edge with SCAN ASYST instrument by taping mode. HPLC analysis was conducted on HPLC system (Model: PU-2080) equipped with a Jasco 2075/2070 UV detector. Methanol was used as mobile phase for analysis with a flow rate of 1.0 mL min-1. The chromatographic separation was done through a C18 column (4.6 mm × 250 mm) and injection volume was 20.0 μL. The chromatographic calculations were done using Borwin software. The electrochemical measurements were carried out on the electrochemical work station [SP-200 (SN 0437)], EC-Lab for windows v10.40 (software) at room temperature. A conventional three electrode system was used for the measurement, which involved an unmodified or modified GCE, a platinum wire counter electrode and a saturated calomel reference electrode.

2.3. Preparation of glycidoxypropyl trimethoxysilane functionalized CNT (GFC)

Mesoporous silica was effectively coated on MWCNT based on the previously reported procedure [16]. A mixture of MWCNT (50.0 mg) and CTAB (0.90 g) were dispersed in deionised water and was sonicated for 1 h. About 40.0 mL of anhydrous ethanol was then added and was further subjected to sonication of 30 min to get a stable dispersion. After immediate addition of 2.0 mL of $NH_3.H_2O$, 2.5% ethanolic solution of TEOS was added as drop wise to the solution with constant stirring for about 12 h. The resultant solution was centrifuged and washed. The surfactant CTAB from the surface of GFC was removed by washing with ethanolic solution of ammonium nitrate by ion exchange mechanism. 0.1 g of the obtained MWCNT@SiO_2 is refluxed with 50 mM of GLYMO in absolute ethanol under N_2 atmosphere for 24 h. The obtained GFC was filtered washed with ethanol and dried at 80 °C [20].

2.4. Synthesis of vinyl functionalized GFC

In brief, 10.0 mg of GFC was dispersed in 10.0 mL AA and was sonicated for 1 h. The resultant homogeneous mixture was continuously stirred at 70 °C for 24 h. Then mixture was centrifuged and washed with ethanol, the product was dried under vacuum to obtain vinyl functionalized GFC (GFC-CH=CH_2).

2.5. Synthesis of MIP

The schematic representation of the formation of MIP on the surface of GFC-CH=CH_2 is given Scheme 1. GFC-CH=CH_2 (2.0 g) was

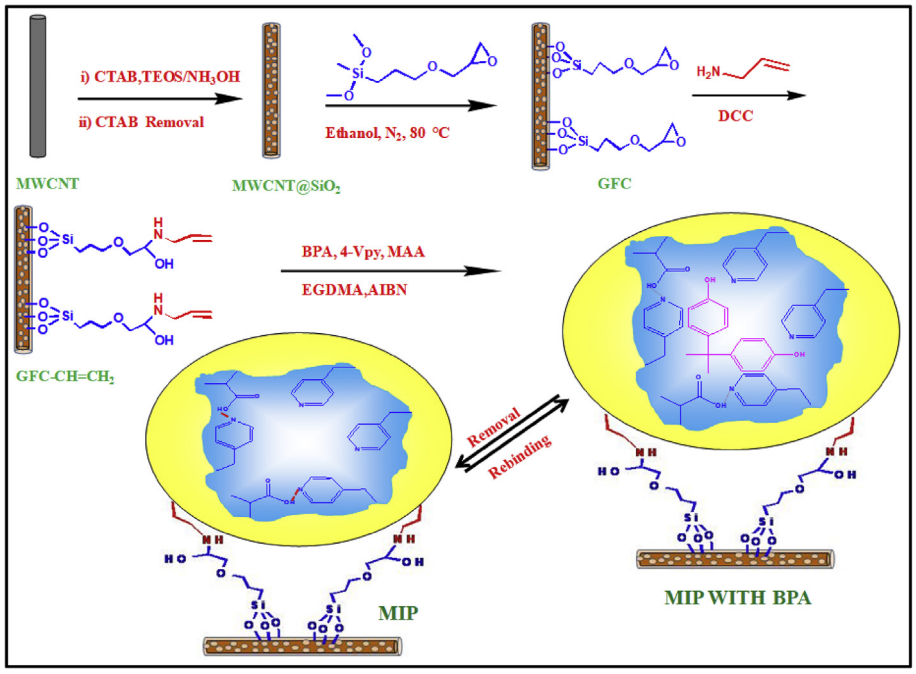

Scheme 1. Synthesis of MIP.

stirred in a round bottom flask containing a mixture of 50.0 mL acetonitrile and 5.0 mL toluene in N_2 atmosphere. The pre-polymerization mixture of template (1.0 mmol) with the functional monomers MAA (2.0 mmol) and 4-VPy (4.0 mmol) in a solvent of N, N – dimethyl formamide was added to the above reaction. EGDMA (24.0 mmol) and initiator (AIBN) were also added. The polymerization was carried out at 70 °C for 16 h. The resultant product, MIP with BPA was centrifuged and washed with ethanol to remove the unreacted reagents. Finally BPA was removed by soxhlet extraction with a mixture of methanol and acetic acid (9:1) so as to obtain BPA imprinted polymer (MIP). After each set of Soxhlet washing, the solution was examined by HPLC-UV analysis and the washing continued till the complete removal of BPA. The obtained MIP was then dried under vacuum at 80 °C. NIP was prepared by the same procedure without the template.

2.6. Electrochemical measurements

Prior to modification, the bare GCE was polished with an abrasive paper and alumina slurry. The synthesized MIP (0.20 g) was ultrasonically mixed with 5.0 mL of 0.10 M acetic acid solution containing 0.5% chitosan (CHI) for 15 min to get a homogenous mixture. 5.0 μL of the resulting suspension was dropped on the surface of the cleaned GCE with a micropipette, which was then dried in air to prepare MIP/GCE. The NIP/GCE sensor was prepared by the same procedure using NIP instead of MIP. Differential pulse voltammograms were recorded by scanning the potential from 0.10 V to 1.0 V. The parameters of DPV containing, pulse amplitude and pulse width were adjusted at 50.0 mV and 0.05 s, respectively.

2.7. Real sample analysis

The real sample solution was prepared according to the previous reports with a few modifications [21]. Plastic baby bottle samples from local supermarket were rinsed successively with ethanol, ultrapure water, and then dried under vacuum for 1 h. After comminuted into small pieces by scissors, the plastic baby bottles (10.0 g) were loaded into a beaker containing 50.0 mL ethanol, and then were stirred at 55 °C for 24 h in order to extract BPA. After cooling to room temperature, the mixture was filtered with 0.45 μm filter membrane and was concentrated to 5.0 mL. After that, the solution was diluted to 500.0 mL with PBS (pH 7.0) solution and was determined with the MIP/GCE.

3. Results and discussion

3.1. Optimization of monomer ratio

Monomer ratios were optimized by measuring the current response of the polymers (MIP), prepared by using different ratios of monomers by CV analysis in PBS solution of BPA. In 1:1 ratio of MAA and 4-Vpy, the current response was lowered due to the absence of imprinting cavies, since MAA preferably form hydrogen bond with 4-Vpy than BPA. Polymer prepared by 2:1 ratio of MAA: 4-Vpy, in addition to the H-bonding between MAA and 4-Vpy, imprinting interaction is also possible by –COOH group of MAA and hydroxyl group of BPA. The H-bonding between MAA and 4-Vpy provides a specific orientation by allowing π-π stacking interaction between 4-Vpy and BPA. Polymer obtained from 1:2 MA A and 4-Vpy, the pyridinyl ring offers H-bonding interaction to BPA. Phenolic OH group is acidic in nature so 4-Vpy is a better candidate to offer H-bonding than MAA [22]. An increased current response was obtained in third polymer (1:2 MA A and 4-Vpy) is due to the presence of specific binding sites in the polymer network. The molecular recognition is the resultant of H-bonding between 4-Vpy and BPA and the π-π stacking interaction of 4-Vpy which is in H-bonding with MAA. The polymers prepared by the monomer ratio 1:2 (MAA: 4-Vpy) was used in the entire studies.

3.2. Characterization of fabricated material

3.2.1. FTIR and Raman analysis

The FTIR spectra of MWCNT, MWCNT@SiO_2, GFC-CH=CH_2, MIP with BPA, MIP and NIP are given in Fig. 1. The spectrum of

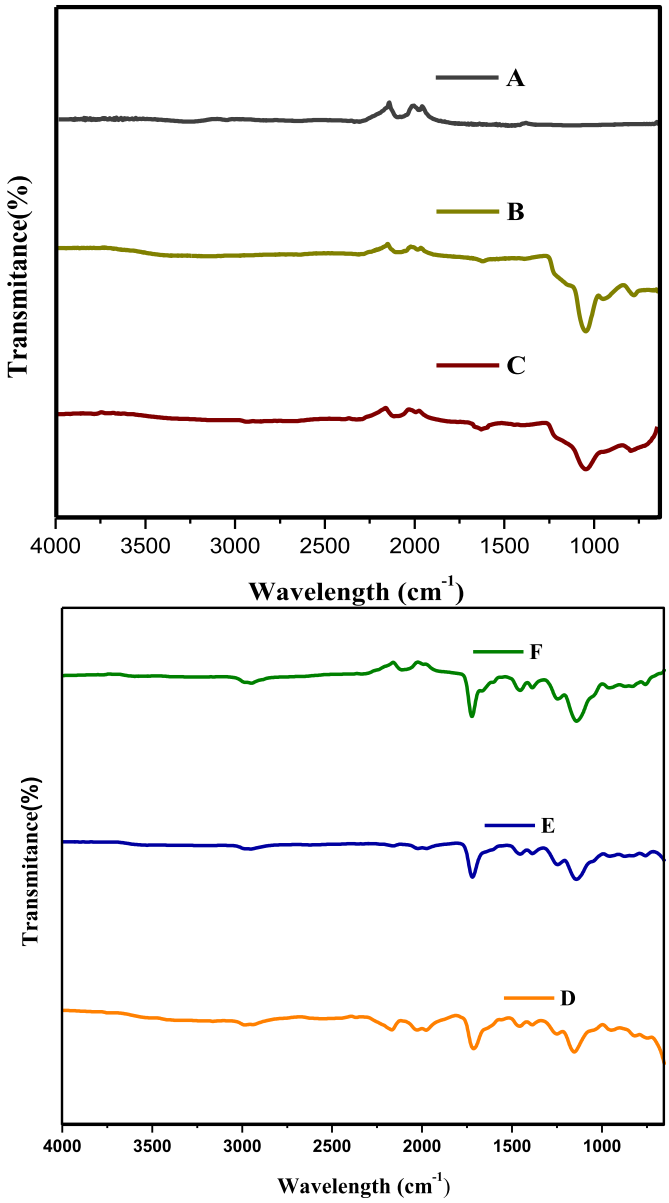

Fig. 1. FTIR spectra of (A) MWCNT, (B) MWCNT@SiO_2, (C) GFC-CH=CH_2, (D) MIP with BPA, (E) MIP and (F) NIP.

MWCT@SiO_2 indicates significant bands at 1082, 959 and 802 cm^{-1}, respectively for Si-O-Si, Si-OH and Si-O stretching vibrations [17,23]. In the GFC-CH=CH_2 spectrum, the peak at 1629 cm^{-1} was ascribed to C=C stretching and absence of Si-OH stretching band at 959 cm^{-1} confirms the reaction at silanol. Bands at 1658 and 1618 cm^{-1} attributed to the N-H stretching vibrations which indicated the effective grafting of AA on GFC [24]. The spectrum of MIP with BPA, MIP and NIP possesses C=C and C=N stretching vibrations around 1600-1400 cm^{-1} ascribed to the presence of vinyl pyridine moiety [25]. On comparing MIP and NIP, we can notice the similar chemical nature of these two types of polymers in which the characteristic interaction of BPA is missing. A band at 1729 cm^{-1} is attributed to the carboxylic O-H stretching vibrations of MAA. In Fig. 1E, the band corresponds to C-H stretching of benzene ring appeared around 2050 cm^{-1} in MIP with BPA was disappeared which confirmed the removal of BPA.

The Raman spectra of MWCNT and MWCNT@SiO_2 are given in Fig. S1. The spectrum of MWCNT shows the characteristic D band appearing at 1350 cm^{-1} related to the non crystalline carbon species, G band at 1580 cm^{-1} due to graphitic carbon network and 2D band at 2700 cm^{-1}, represents a long range order in MWCNT [26]. No significant band shift is observed in the spectrum of silica coated MWCNT indicating the non-covalent interaction between silica network and CNTs [27]. Also an up shift of about 40–50 cm^{-1} for the D and G bands was observed for silica coated MWCNT compared with MWCNT, which confirms the effective coating of silica on MWCNTs.

3.2.2. XRD analysis

Fig. 2 represents the X-ray diffractograms of MWCNT, MWCNT@SiO_2, GFC-CH=CH_2, MIP with BPA, NIP and MIP. For MWCNT, a sharp diffraction peak at $2\theta = 26.4^\circ$ (0,0,2) and a broad peak at 43.3° (1,0,0) attributed to the hexagonal graphite structure of MWCNT [26]. The characteristic peak of MWCNT at 26.4°was shifted and broadened for MWCNT@SiO_2, which confirmed the perfect coating of amorphous silica on MWCNT [28]. The broadening of hump in the diffraction pattern of GFC-CH=CH_2 suggested the grafting of AA. The broad peaks at 2θ 15° and 2θ 30° of MIP were disturbed by presence of the BPA. After the removal of BPA, the crystalline nature of MIP is increased. The more degree of order of MIP is due to the presence of specific binding sites on the surface of MIP. The more amorphous nature of NIP is due to the lack of specific imprinting cavities.

3.2.3. Morphological characterization

The surface morphology of fabricated samples was explored with scanning electron microscope. The SEM images of MWCNT, MWCNT@SiO_2, GFC-CH=CH_2, NIP and MIP are represented in Fig. 3 where, as expected significant changes in the surfaces are noticed. In Fig. 3A, the MWCNT shows an average diameter in 50–80 nm. After coating silica the diameter of MWCNT seemed to be increased, indicating the successful coating, as shown in Fig. 3B.The change in morphological features of Fig. 3C confirms the grafting of allyl amine. On comparing the image of NIP and MIP [Fig. 3D and (E)], the image of the former is more uniform in nature ascribed to the absence of imprinting sites. Micrographs of MIP and NIP clearly give the morphological differences even though chemical nature is

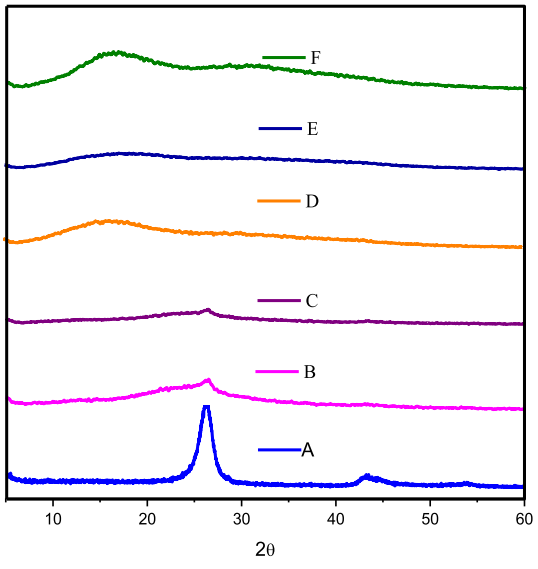

Fig. 2. X-ray diffractograms of (A) MWCNT, (B) MWCNT@SiO_2, (C) GFC-CH=CH_2, (D) MIP with BPA, (E) NIP and (F) MIP.

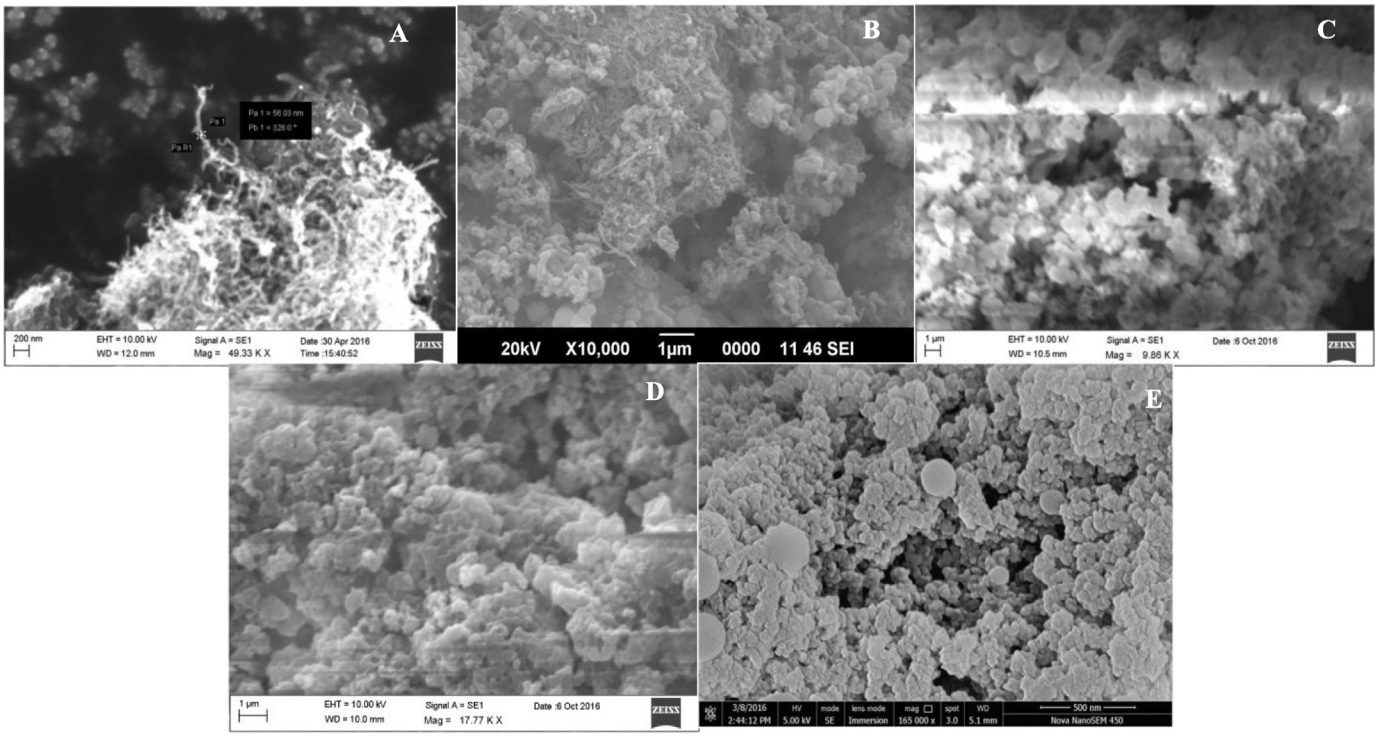

Fig. 3. The SEM images of (A) MWCNT, (B) MWCNT @SiO_2, (C) GFC-CH=CH_2, (D) NIP and (E) MIP.

same. The crumpled spots seen on MIP unveil the presence of specific binding sites for BPA. The increased porous surface morphology enhances the electro catalytic action of MIP.

The AFM images of MWCNT, MWCNT@SiO_2, GFC-CH=CH_2, MIP, MIP with BPA and NIP are shown in Fig. 4. The 3D image of MWCNT displays a tubular architecture with agglomerated topography. On comparing AFM images of MWCNT and MWCNT@SiO_2 the change in surface appearance to spindle shaped morphology is attributed to the successful silylation. In GFC-CH=CH_2, the smoothening of the spindles compared to MWCNT@SiO_2 indicates the surface modification due to allyl grafting. On comparing the MIP with BPA and MIP, the former appears to be swollen and the increase in broadness could explain the interaction of BPA on MIP network. The regular and uniform spikes present on MIP are attributed to the presence of specific binding sites.

3.3. Cyclic voltammetric characterization of different electrodes

The CV of ferricyanide was used to characterize the electrochemical behaviour of bare and modified electrodes. Fig. 5a Shows the CV response of BGC, NIP/GC and MIP/GC in an electrolytic solution of 1.0 mM $K_3[Fe(CN)_6]$ and 0.1 M $KClO_4$. A couple of redox peaks with a peak potential separation (ΔEp) of 113.3 mV was obtained for the bare GCE. After modifying the electrode with MIP, the peak potential separation (ΔEp) is 95.1 mV which is due to the excellent reversibility of the MIP sensor electrode. The significant increase in the redox peak current indicates the excellent electrical conductivity and larger surface area of the MIP sensor electrode. For NIP sensor, the redox peak current is greatly declined. This might be due to the absence of electro active cavities (MIP cavities) on NIP sensor compared to MIP. A shift in potential was observed for MIP and NIP compared to bare GCE is due to the presence of polymeric material containing conducting MWCNT. It is reported [29] that the shift in potential is an indication of more reversible system caused by the effectiveness of electron transfer.

The interference properties of different electrodes were investigated using electrochemical impedance spectroscopy (EIS). Fig. 5b represents the Nyquist plot of BGC, NIP/GCE and MIP/GCE in a solution of 1.0 mM $K_3[Fe(CN)_6]$ and 0.1 M KCl. A typical Nyquist represents, a semicircle portion indicating the electron transfer resistance at higher frequency and a linear portion corresponds to diffusion limited process at lower frequency. When compared to BGC, MIP/GCE exhibits reduced semicircular domain. A straight line obtained for MIP/GCE indicates its least electron transfer resistance and improved diffusion rate of solution towards the electrode interfaces. The results also indicated that MIP/GCE possesses a higher conductivity than BGC.

3.4. The response of sensor to BPA

The electrochemical behaviour of different modified electrodes (BGC, MIP/GCE and NIP/GCE) is also investigated in a 2.0 μM BPA solution of pH (7.0) phosphate buffer at a scan rate of 50 mV s^{-1} using cyclic voltammogram and results are shown in Fig. 6a. The major redox peak appears at around 250 mV in anodic sweep and the corresponding reduction peak in cathodic sweep is obtained at about 180 mV. The low peak height of NIP/GCE suggests the poor electro catalytic activity of NIP/GCE sensor. The NIP/GCE gave a weak redox response compared to MIP/GCE. Even though NIP has no cavity to bind BPA, it contains the similar functionalities of MIP. The presence of specific imprinting sites enhances the current response of BPA in MIP/GCE. NIP is also containing conducting MWCNT, so there also takes place the electrochemical reaction. But due to the absence of complimentary sites, the current response is very poor. The enhanced redox response of MIP/GCE indicates the presence of complimentary cavities. MIP is also compared with BGC (control). BGC also gives a weak repose to BPA. The BGC gives only a broad anodic peak. The absence of reduction peak indicates the irreversible nature of electrochemical reaction of BPA.

The possible electrochemical sensing mechanism of BPA on MIP/

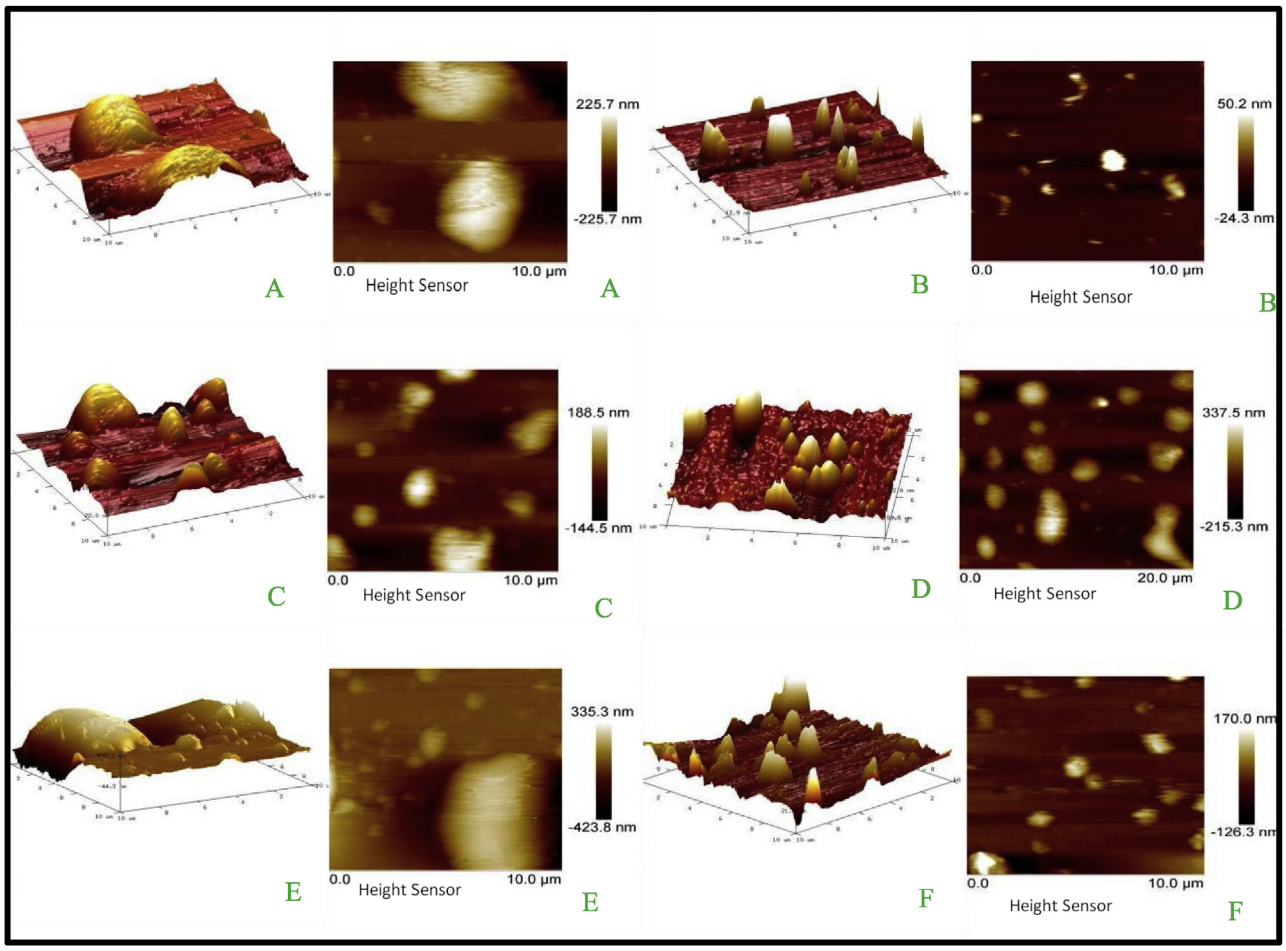

Fig. 4. The AFM images of (A) MWCNT, (B) MWCNT @SiO_2, (C) GFC-CH=CH_2, (D) MIP, (E) MIP with BPA and (F) NIP.

GCE follows four electrons and four proton process as explained in the earlier report [30]. The electro oxidation of BPA can be illustrated as follows.

Electrochemical characterization of MIP in PBS solution (Fig. 6b) shows a reduction peak at 185 mV implies the characteristic reduction nature of the electrode modified with MIP on MWCNT. On interacting with BPA solution, the characteristic peak of the electrode increases due to the electrochemical reaction of BPA taking place at the imprinted site. The peak obtained for MIP/GCE in PBS solution indicates the reducing nature of the polymer on MWCNT and the value is enhanced in the presence of BPA.

3.5. Optimization of electrochemical protocol

The electrochemical behaviour of BPA was explored as a function of pH using a series of phosphate buffer and is shown in Fig. 7a. The value of pH was varied between 4.0 and 10.0. With increase in pH from 4.0 to 7.0, the oxidation current increased and reached a maximum value at pH 7.0, after that it decreased with further increase in pH from 8.0 to 10.0. Maximum anodic peak current was observed at pH 7.0 and was selected as optimum pH. The strong protonation ability of BPA declines the interaction of BPA with MIP under harsh acidic conditions. The maximum current response was obtained at pH 7.0, below the pKa of BPA (9.73). Moreover the hydroxyl groups in undissociated BPA can form hydrogen bond with pyridinyl group in the polymer matrix than the dissociated ion form.

In order to further improve the analytical procedure with the aim of allowing most optimized experimental conditions for the sensing of BPA, the incubation time was also explored and represented in Fig. 7b. An optimized incubation time of 20 min was applied for subsequent electrochemical analysis.

3.6. Analytical applications of MIP/GCE

Fig. 8 depicts the typical differential pulse voltammetric profile resulting from the addition of BPA made into pH 7.0 buffer solution over a concentration ranges from 1.0×10^{-10} to 4.0×10^{-4} M using the modified GCE. A well defined and sharp oxidation peak was obtained for BPA at 217.9 mV. A linear dynamic range from 1.0×10^{-10} to 4.0×10^{-4} M with a calibration equation of $I_{BPA} = 20.978 + 0.951\ C_{BPA}$ ($R^2 = 0.998$) is obtained. A comparison of MIP/GCE with other reported electrodes modified for the detection of BPA is listed in Table 1. Compared to reported literature, the fabricated sensor shows a large linear range and low detection limit.

3.7. Selectivity

Selectivity was studied by testing the structural analogues of BPA including BPF, Ph, and DHB, represented in Fig. 9. It was seen that the current response of MIP/GCE towards BPA is much greater than that generated by the analogues of tenfold concentration. The outstanding specificity could be ascribed to the complimentary MIP

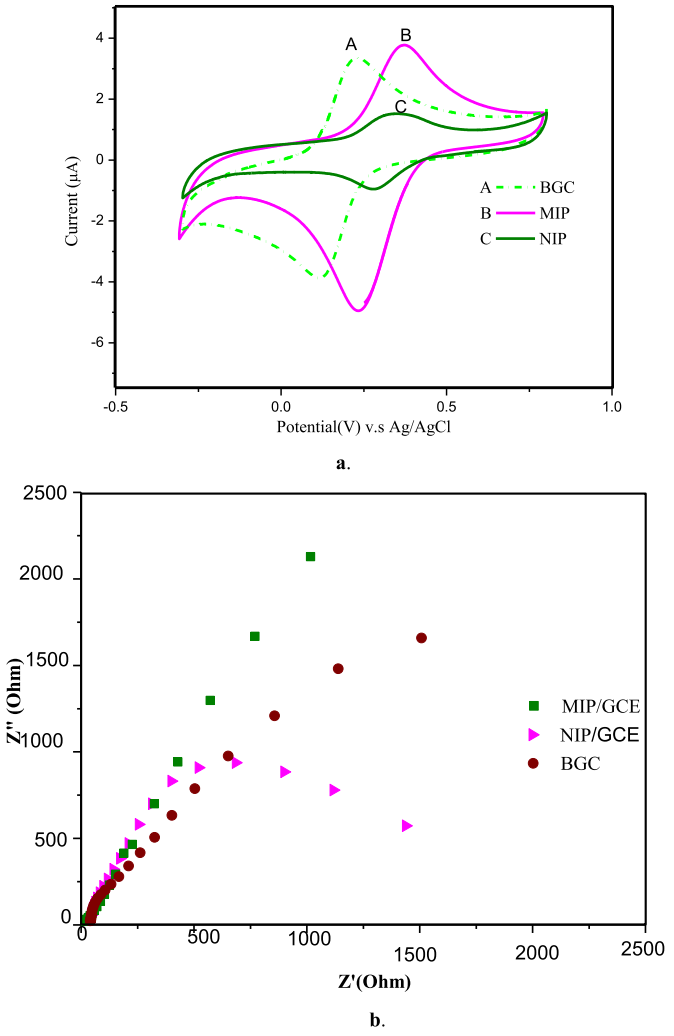

Fig. 5. **a**. CV response of BGC, NIP/GC and MIP/GC in an electrolytic solution of 1.0 mM $K_3[Fe(CN)_6]$ and 0.10 M KCl. **b**. Nyquist plot of BGC, NIP and MIP in a solution of 1.0 mM $K_3[Fe(CN)_6]$ and 0.1 M KCl.

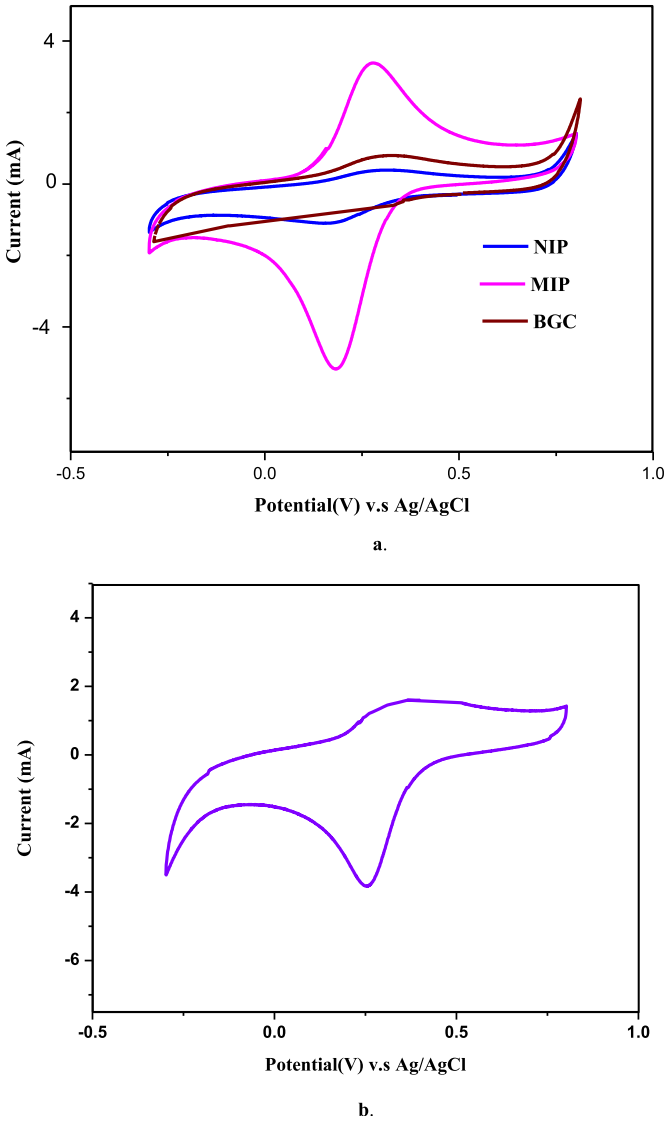

Fig. 6. **a**. CV response of MIP/GCE, NIP/GCE and BGC in PBS solution of BPA. **b**. CV response of MIP/GCE in PBS solution.

cavities in the polymer for mimicking the structure of BPA via the interaction between the functional monomers and template.

In addition, the specificity of the sensor was also determined. The current response of BPA in a solution containing NH_4^+, Ca^{2+}, Na^+, K^+, Cl^-, NO_3^- with a concentration tenfold amount than that of BPA was tested. The electrical response of BPA is seemed to be not affected indicating the good specificity of the template towards MIP.

3.8. Stability, repeatability and reproducibility

The stability of the prepared sensor was evaluated by checking the current response of 5×10^{-9} M BPA solution for consecutive 10 days with the electrode being retained at room temperature. The MIP/GCE can retain 94.3% of its initial response after 10 days. The repeatability of MIP sensor was examined by measuring the electrochemical response of 5.0×10^{-9} M concentration of BPA for 5 replicate measurements using the same MIP/GCE sensor. After each measurement BPA was extracted using methanol: acetic acid (9:1) solution.The relative standard deviation (RSD) value of 2.4% ascribed to the good repeatability of the MIP/GCE sensor. The reproducibility of the MIP/GCE was evaluated by constructing five MIP/GCE sensors and the current response to 5.0×10^{-6} M concentration of BPA was investigated. The obtained RSD was 2.1% confirming the reproducibility of the fabrication method.

3.9. Determination of BPA in real samples

The MIP/GCE sensor was evaluated towards the determination of BPA in commercially available baby feeding bottle samples. The samples were prepared as described in the experimental section 2.7. HPLC was also performed to detect the content of BPA to testify the accuracy of the proposed method and the results are listed in Table 2. The results obtained from HPLC method and the proposed sensor were in good agreement, reveal the reliability of fabricated sensor in the real life applications. The student t-test is conducted for the comparison of HPLC method with the present method. The results obtained were satisfactory.

4. Conclusions

A selective and sensitive MIP was synthesized and used for modifying GCE for the electrochemical detection of BPA.

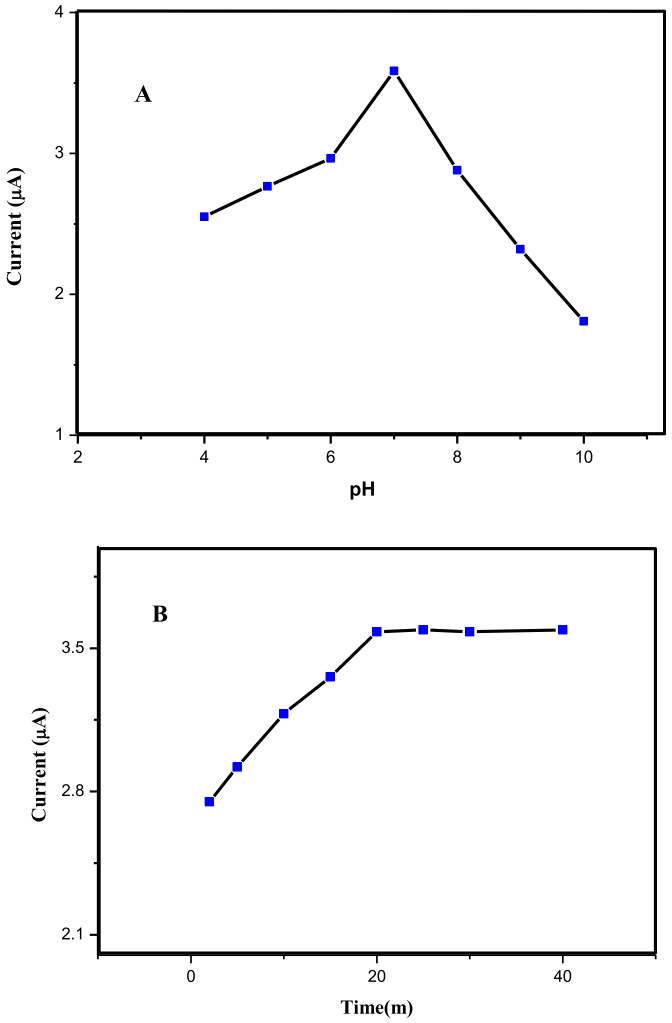

Fig. 7. Influence of (A) pH values and (B) incubation time on the electrochemical responses of the MIP/GCE sensor.

Characterization of MIP using FTIR, Raman, XRD, SEM and AFM techniques confirms the stepwise modification in each stage. CV and DPV were used to characterize the electro-catalytic behaviour of modified GCE. The optimization of pH (7.0) and incubation time (20 m) was achieved during the CV analysis. The increased current observed in MIP/GCE proves the specificity of MIP as adsorption of BPA on the sensor increased, indicating the presence of specific binding sites. A lower detection limit (0.02 nM) and a dynamic linear range obtained during DPV analysis can be concluded to the applicability of the sensor in the analysis of real samples. The results indicate that the proposed sensor could be used for the detection of BPA in various samples including food and water storage bottles.

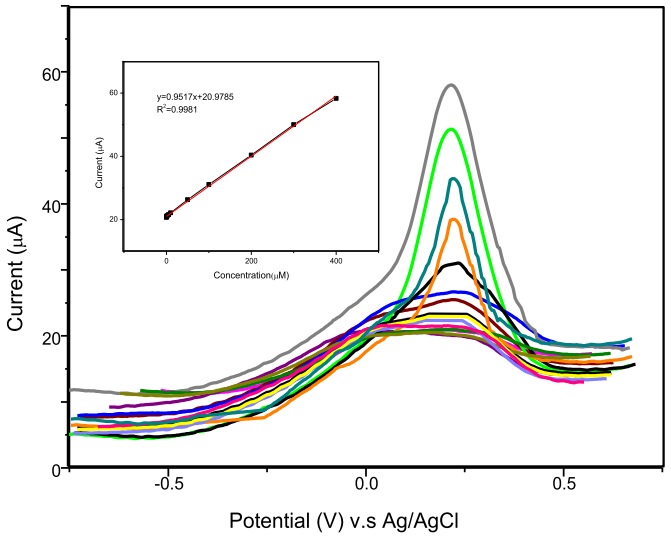

Fig. 8. DPV curves of MIP/GCE sensor in phosphate buffer (pH = 7.0) containing different concentrations of BPA. Inset: Calibration curve of BPA concentration in the range of 1.0×10^{-10} to 4.0×10^{-4} M.

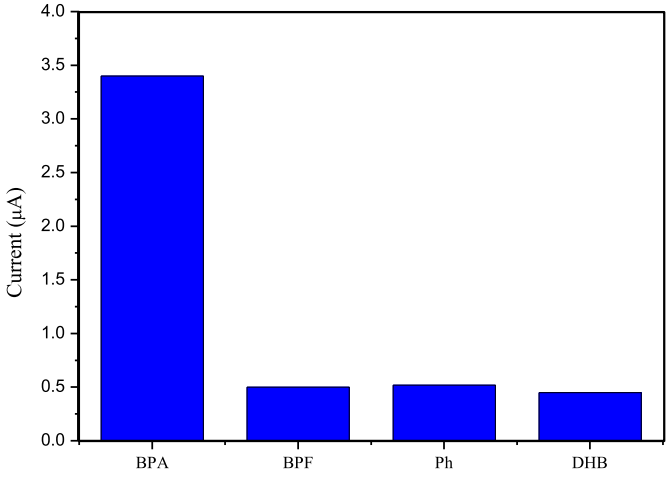

Fig. 9. Comparison of sensing response of BPA with its analogues using MIP/GCE. The concentrations of BPA, bisphenol F (BPF), phenol (Ph), and 1,4-dihydroxybenzene(DHB) were, 5.0×10^{-6}, 5.0×10^{-5}, 5.0×10^{-5} and 5.0×10^{-5} M, respectively.

Table 2
Determination of BPA in real samples (Baby bottle).

Sample	HPLC Method[a]		Present Method[a]	
	Amount Found (nM)	RSD (%)	Amount Found (nM)	RSD (%)
1	57.51 ± 1.84	3.20	56.23 ± 1.40	2.50
2	89.65 ± 2.06	2.30	85.54 ± 1.45	1.70
3	63.25 ± 1.17	1.75	62.21 ± 1.24	2.00
4	92.87 ± 2.41	2.60	93.31 ± 1.11	1.20

[a] Average of five measurements.

Table 1
A comparison of linear range and detection limit for BPA by MIP/GCE with the other reported literature values of sensors.

Type of Electrode	Technique	Linear range (M)	Detection Limit (M)	Reference
AuNPs/SGNF/GCE	LSV	$5.0 \times 10^{-9} - 1.0 \times 10^{-6}$	3.5×10^{-8}	[30]
CTAB/CPE	CV	$6.0 \times 10^{-7} - 1.0 \times 10^{-4}$	1.0×10^{-7}	[21]
MIP-GR/ABPE	Derivative voltammetry	$8.0 \times 10^{-9} - 1.0 \times 10^{-6}$; $1.0 \times 10^{-6} - 2.0 \times 10^{-5}$	6.0×10^{-9}	[31]
ZrO2(20%)/Nano-ZSM-5/GCE	DPV	$6.0 \times 10^{-9} - 6.0 \times 10^{-4}$	3.0×10^{-9}	[32]
MIPMSs/CPE	CV	$1.0 \times 10^{-11} - 8.0 \times 10^{-7}$	2.8×10^{-12}	[33]
SPA-MIP	CV	$1.0 \times 10^{-7} - 5.0 \times 10^{-4}$	3.2×10^{-8}	[34]
MIP/GCE	DPV	$1.0 \times 10^{-10} - 4.0 \times 10^{-4}$	0.2×10^{-11}	Present Work

Acknowledgements

The authors are thankful to the Head, Department of Chemistry, University of Kerala for providing necessary laboratory facilities. The (Athira V.S. and Chithra Sekhar V) are thankful to University of Kerala, Trivandrum, India for providing assistance in the form of research fellowship.

Appendix A. Supplementary data

Supplementary data related to this article can be found at https://doi.org/10.1016/j.polymer.2018.05.052.

References

[1] S. Flint, T. Markle, S. Thompson, E. Wallace, Bisphenol A exposure, effects, and policy: a wildlife perspective, J. Environ. Manag. 104 (2012) 19–34.
[2] S. Soriano, C. Ripoll, P. Alonso-Magdalena, E. Fuentes, I. Quesada, A. Nadal, J. Martinez-Pinna, Effects of Bisphenol A on ion channels: experimental evidencnce and molecular mechanisms, Steroids 111 (2016) 12–20.
[3] D. Pfeifer, Y.M. Chung, M.C.-T. Hu, Effects of low-dose bisphenol a on DNA damage and proliferation of breast cells: the role of c-Myc, Environ. Health Perspect. 123 (2015) 1271–1279.
[4] K.V. Ragavan, N.K. Rastogi, M.S. Thakur, Review-Sensors and biosensors for analysis of bisphenol-A, Trends Anal. Chem. 52 (2013) 248–260.
[5] Z. Zheng, Y. Du, Z. Wang, Q. Feng, C. Wang, Pt/graphene–CNTs nanocomposite based electrochemical sensors for the determination of endocrine disruptor bisphenol A in thermal printing papers, Analyst 138 (2013) 693–701.
[6] E. Mazzotta, C. Malitesta, E. Margapoti, Direct electrochemical detection of bisphenol A at PEDOT-modified glassy carbon electrodes, Anal. Bioanal. Chem. 405 (2013) 3587–3592.
[7] K. Haupt, K. Mosbach, Molecularly imprinted polymers and their use in biomimetic sensors, Chem. Rev. 100 (2000) 2495–2504.
[8] K. Ensing, T. Boer, Tailor-made materials for tailor-made applications: application of molecular imprints in chemical analysis, Trends Anal. Chem. 18 (1999) 1271–1279.
[9] V. Pichon, F. Chapuis-Hugon, Role of molecularly imprinted polymers for selective determination of environmental pollutants—a review, Anal. Chim. Acta 622 (2008) 48–61.
[10] Y. Lv, T. Tan, F. Svec, Research review paper-Molecular imprinting of proteins in polymers attached to the surface of nanomaterials for selective recognition of biomacromolecules, Biotechnol. Adv. 31 (2013) 1172–1186.
[11] Y. Wang, Y. Yang, L. Xu, J. Zhang, Bisphenol A sensing based on surface molecularly imprinted, ordered mesoporous silica, Electrochim. Acta 56 (2011) 2105–2109.
[12] B. Liu, H.T. Lian, J.F. Yin, X.Y. Sun, Dopamine molecularly imprinted electrochemical sensor based on graphene–chitosan composite, Electrochim. Acta 75 (2012) 108–114.
[13] J. Huang, X. Xing, X. Zhang, X. He, Q. Lin, W. Lian, H. Zhu, A molecularly imprinted electrochemical sensor based on multiwalled carbon nanotube-gold nanoparticle composites and chitosan for the detection of tyramine, Food Res. Int. 44 (2011) 276–281.
[14] C. Zhanga, S. Sia, Z. Yan, Design of molecularly imprinted TiO2/carbon aerogel electrode for the photoelectrochemical determination of atrazine, Sens. Actuators, B 211 (2015) 206–212.
[15] H. Dai, D. Xiao, H. He, H. Li, D. Yuan, C. Zhang, Synthesis and analytical applications of molecularly imprinted polymers on the surface of carbon nanotubes: a review, Microchim. Acta 182 (2015) 893–908.
[16] K. Ding, B. Hu, Y. Xie, G. An, R. Tao, H. Zhang, Z. Liu, A simple route to coat mesoporous SiO2 layer on carbon nanotubes, J. Mater. Chem. 19 (2009) 3725–3731.
[17] M. Zhang, Y. Wu, X. Feng, X. He, L. Chen, Y. Zhang, Fabrication of mesoporous silica-coated CNTs and application in size-selective protein separation, J. Mater. Chem. 20 (2010) 5835–5842.
[18] L. Zhang, G. Wang, Z. Xing, Polysaccharide-assisted incorporation of multi-walled carbon nanotubes into sol–gel silica matrix for electrochemical sensing, J. Mater. Chem. 21 (2011) 4650–4656.
[19] H. Chen, O. Jacobs, W. Wu, G. Rüdiger, B. Schädel, Effect of dispersion method on tribological properties of carbon nanotube reinforced epoxy resin composites, Polym. Test. 26 (2007) 351–360.
[20] X. Fei, S. Chen, C. Huang, D. Liu, Y. Zhang, Immobilization of bovine carbonic anhydrase on glycidoxypropyl-functionalized nanostructured mesoporous silicas for carbonation reaction, J. Mol. Catal. B Enzym. 116 (2015) 134–139.
[21] L. Zhu, Y. Cao, G. Cao, Electrochemical sensor based on magnetic molecularly imprinted nanoparticles at surfactant modified magnetic electrode for determination of bisphenol A, Biosens. Bioelectron. 54 (2014) 258–261.
[22] F. Puoci, C. Garreffa, F. Iemma, R. Muzzalupo, U.G. Spizzirri, N. Picci, Molecularly imprinted solid phase extraction for detection of Sudan I in food matrices, Food Chem. 93 (2005) 349–353.
[23] W. Yang, F. Jiao, L. Zhou, X. Chen, X. Jiang, Molecularly imprinted polymers coated on multi-walled carbon nanotubes through a simple indirect method for the determination of 2,4-dichlorophenoxyacetic acid in environmental water, Appl. Surf. Sci. 284 (2013) 692–699.
[24] T.S. Anirudhan, S. Alexander, Design and fabrication of molecularly imprinted polymer-based potentiometric sensor from the surface modified multiwalled carbon nano tube for the determination of lindane(γ-hexachlorocyclohexane), an organochlorine pesticide, Biosens. Bioelectron. 64 (2015) 586–593.
[25] G. Bayramoglu, M.Y. Arica, Synthesis of Cr (VI)-imprinted poly(4-vinyl pyridine-co-hydroxyethyl methacrylate) particles: its adsorption propensity to Cr(VI), J. Hazard Mater. 187 (2011) 213–221.
[26] S. Karimifard, M.R.A. Moghaddam, Enhancing the adsorption performance of carbon nanotubes with a multistep functionalization method: optimization of Reactive Blue 19 removal through response surface methodology, Process Saf. Environ. Protect. 99 (2016) 20–29.
[27] X. Lu, H. Liu, C. Deng, X. Yan, Facile synthesis and application of mesoporous silica coated magnetic carbon nanotubes, Chem. Commun. 47 (2011) 1210–1212.
[28] M. Kim, J. Hong, J. Lee, C.K. Hong, S.E. Shima, Fabrication of silica nanotubes using silica coated multi-walled carbon nanotubes as the template, J. Colloid Interface Sci. 322 (2008) 321–326.
[29] F.R. Caetanoa, L.B. Felippea, A.J.G. Zarbinb, M.F. Bergaminia, L.H. Marcolino-Juniora, Gold nanoparticles supported on multi-walled carbon nanotubes produced by biphasic modified method and dopamine sensing application, Sensor. Actuator. B Chem. 243 (2017) 43–50.
[30] X. Niua, W. Yanga, G. Wangb, J. Rena, H. Guoa, J. Gaoa, A novel electrochemical sensor of bisphenol A based on stacked graphene nanofibers/gold nanoparticles composite modified glassy carbon electrode, Electrochim. Acta 98 (2013) 167–175.
[31] P. Deng, Z. Xu, Y. Kuang, Electrochemical determination of bisphenol A in plastic bottled drinking water and canned beverages using a molecularly imprinted chitosan–graphene composite film modified electrode, Food Chem. 157 (2014) 490–497.
[32] B. Kaura, R. Srivastava, B. Satpatib, ZrO2 supported Nano-ZSM-5 nanocomposite material for the nanomolar electrochemical detection of metol and bisphenol A, RSC Adv. 6 (2016) 65736–65746.
[33] Y. Liu, L. Zhang, N. Zhao, Y. Han, F. Zhao, Z. Peng, Y. Li, Preparation of molecularly imprinted polymeric microspheres based on distillation-precipitation polymerization for ultrasensitive electrochemical sensor, Analyst 142 (2017) 1091–1098.
[34] Y. Wang, Y. Yang, L. Xu, J. Zhang, Bisphenol A sensing based on surface molecularly imprinted, ordered mesoporous silica, Electrochim. Acta 56 (2011) 2105–2109.